RSC Advances

ROYAL SOCIETY OF CHEMISTRY

www.rsc.org/advances

Journal Name

Cite this: DOI: 10.1039/c0xx00000x

www.rsc.org/xxxxxx

ARTICLE TYPE

Hexahapto-Chromium Complexes of Graphene: A Theoretical Study

Song Liu,[a] Yu Lei,[a,b] Yingzi Li,[a] Tao Zhang,[a] Huan Wang[a] and Yu Lan[a,*]

Received (in XXX, XXX) Xth XXXXXXXXX 20XX, Accepted Xth XXXXXXXXX 20XX
DOI: 10.1039/b000000x

Chromium fragments coordinated with graphene provide a potentially powerful method for the modification of graphene. The newly reported density functional theory method, M11-L, is employed to elucidate the coordination of chromium fragments with graphene. Oligoacenes were chosen to model graphene. The radii of the centrosymmetric oligoacenes were systematically increased to find the limit required to model graphene. Meta-trisubstituted benzene coordinated chromium fragments were employed to study the electronic effect of the complexation of chromium with graphene. The movement and arrangement of the chromium fragments on graphene is also studied.

Introduction

Graphene, a single atomic sheet of graphite, is a two-dimensional planar sheet of sp^2 hybridized carbon atoms.[1–2] Single-layer graphene was first isolated in the laboratory in 2004 by Geim and co-workers.[3] Since then, graphene has become widely used because its delocalized π electron structure provides the basis for unique physical phenomena.[4–6] Graphene has great potential as an electronic material because its unique Fermi surface and ballistic conductance yield excellent transport properties. However, graphene by itself cannot be directly used as the core component in conventional field-effect transistors because it does not have an energy gap.[7–8] Therefore, functionalization of graphene is an area that has been given large attention.[9-10] Meanwhile, methods on how to controllably functionalize graphene[11] and how to efficiently produce single layer graphene sheets[12] are two main challenges in the extension of the applications of graphene.

Modification of pristine graphene is one of the most important fields in graphene chemistry.[13] Graphene can be defined as alternating multiple conjugated double bonds and the conduction and valence bands (the highest occupied molecular orbital (HOMO) and the lowest unoccupied molecular orbital (LUMO)) that cross at the Dirac point.[14-15] The Diels-Alder reaction is a simple and efficient way to functionalize graphene. Graphene can react with both diene and dienophile. Graphene is very versatile and it can be prepared under very mild conditions.[16-18] 1,3-dipolar cycloaddition acts as a powerful tool for functionalizing graphene.[19-20] Azomethine ylide is often used as a substrate to react with graphene, which has generated some potential electronic materials. Some other cycloaddition reactions have also been used to functionalize graphene, such as nitrene addition[21] and diazonium coupling.[22] The covalent bonds that form reactions can be used to generate aryl-graphene,[23-26] graphene oxide,[27-30] graphane[31-32] and fluorographene.[33-36] The adsorption of metal atoms on graphene is another method for modifying graphene, except for the organic synthesis. The interactions between the metals and graphene were studied theoretically.[37] Bangert and co-workers used high-resolution scanning transmission electron microscopy and found that chromium atoms interacted more strongly with a clean single-layer graphene than with other transition metals.[38-39]

Organic reactions can easily modify pristine graphene and the sp2 hybridized carbon atoms can usually be converted to sp3 hybridized carbon. In these cases, the conjugated double bonds are irreversibly broken. Therefore, the material being fabricated is difficult to control.[40] Recently, Haddon and co-workers reported the first organometallic method to functionalize graphene.[41] As shown in Scheme 1, graphene can react with (η^6-benzene)$Cr(CO)_3$ or $Cr(CO)_6$ in refluxed tetrahydrofuran (THF), and either graphene-Cr(η^6-benzene) or graphene-$Cr(CO)_3$ is generated, respectively. Graphene-chromium complexes can be decomposed by adding mesitylene and the graphene obtained can be reversibly isolated. In the formed graphene-chromium complexes, the conjugated π electrons donate the empty d orbital in chromium and a unique Fermi level electronic structure is obtained. This work introduces a new method for functionalizing graphene, but the interactions between graphene and the coordinated chromium complex were not clear. Calculations using density functional theory (DFT) were performed to investigate the interactions between graphene and the coordinated chromium complex. In the current study, the movement of the chromium complexes on two-dimensional graphene surfaces is explained along with how multiple chromium complexes can coordinate with graphene.

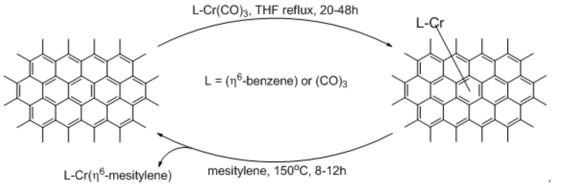

Scheme 1. The formation and decomposition of graphene-chromium complexes.

Computational method

All of the DFT calculations were carried out with the GAUSSIAN 09 program.[42] The hybrid B3LYP functional [43-44] and the combinatorial basis set BSI (the SDD basis set[45-46] was used for chromium and the 6-31G(d) basis set was used for all of the other atoms) were used to optimize the geometries of all of the local minima and saddle points. The relative energies were obtained with a single point calculation using the M11-L[47-48] functional with the combinatorial basis set BSII (the SDD basis set was used for chromium and the 6-311G+(d) basis set was used for all of the other atoms).

Results and discussion

In this study, centrosymmetric oligoacenes (shown in Scheme 2) were employed as a model to study the reactivity of single-layer graphene. The six-membered ring center of the limited oligoacene was set as the reaction point, which could be modeled as a unit of unlimited graphene. The radii of the model oligoacenes were set from **1** to **5** and the relative binding energies for $(C_6H_6)Cr$ and $(CO)_3Cr$ with graphene models **1**–**5** are shown in Figure 1. To begin, benzene, the simplest "oligoacene" (radius = 1) was used. M11-L was used to calculate the binding energy of benzene **1** with $(CO)_3Cr$, giving 37.0 kcal/mol. The binding energy for coronene **2** with $(CO)_3Cr$ was 19.5 kcal/mol, which was 17.5 kcal/mol lower than that for benzene. Information on the geometries of the coordination complexes is given in Scheme 3. The bond length of C(oligoacene)-chromium in complex **7** was 0.17 Å longer than that in complex **6**. When oligoacenes **3**, **4** and **5** were employed as graphene models to calculate the binding energy with $(CO)_3Cr$, the binding energies were 22.3 kcal/mol, 20.7 kcal/mol and 23.0 kcal/mol, respectively. When the radii of the oligoacenes were larger than two, the binding energies for the oligoacenes with $(CO)_3Cr$ were closed and the binding energies with an odd radii oligoacenes were about 3 kcal/mol higher than those with an even radii oligoacenes.

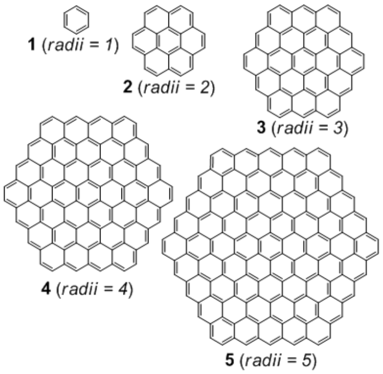

Scheme 2. Centrosymmetric oligoacenes, which were employed to model a single layer of graphene.

The binding energies for $(C_6H_6)Cr$ were also calculated with graphene models **1**–**5** (blue lines in Figure 1). The binding energies for $(C_6H_6)Cr$ with benzene **1** and coronene **2** were 54.8 kcal/mol and 34.5 kcal/mol, respectively. When the radius was larger than 3, the binding energies were between 42.5 kcal/mol and 38.8 kcal/mol, displaying the same trend as $(CO)_3Cr$. The B3LYP calculations gave the same trend as the binding energies (dashed lines in Figure 1). However, for oligoacenes **3**–**5**, the binding energies calculated with the B3LYP functional were about 10 kcal/mol lower than those calculated using the M11-L functional because B3LYP functional underestimate the back-donation of oligoacenes.[47-48]

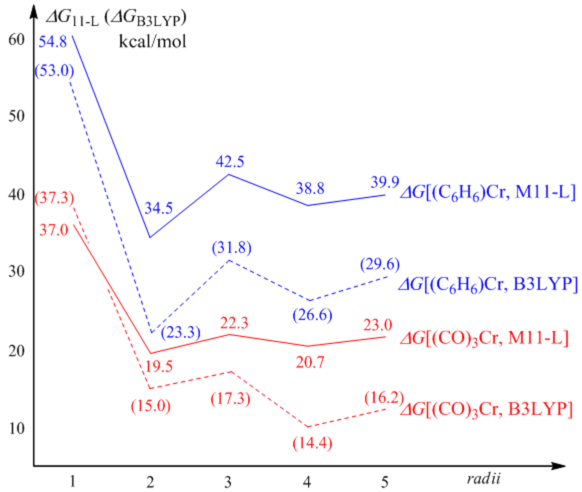

Figure 1. Binding energies for graphene models **1**–**5** with either $(CO)_3Cr$ or $(C_6H_6)Cr$. The closed lines were obtained using the M11-L functional and the dashed lines are the B3LYP calculated values. The values are given in kcal/mol.

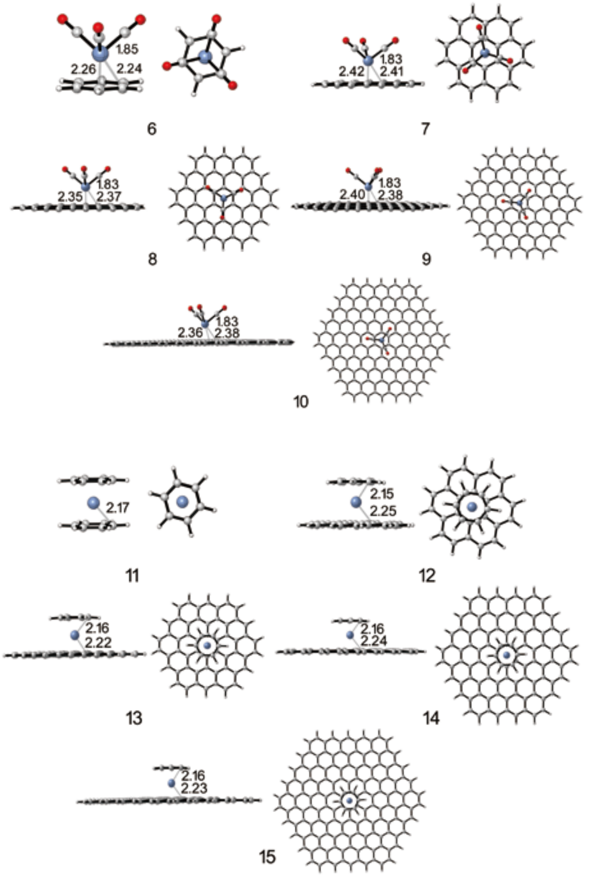

Scheme 3. The geometries of graphene models **1**–**5** bound with either $(CO)_3Cr$ or $(C_6H_6)Cr$, calculated using the M11-L functional.

The DFT calculations showed that when the radius was larger than **2**, the binging energies were vibrative, but the changes in the binding energies were lower than 5 kcal/mol. Therefore, complex **3** and its derivatives were chosen to model graphene and to study the reactivities.

The meta-trisubstituted benzene coordinated chromium fragment, **16** was chosen to study the binding energy with graphene model **3**. The B3LYP and M11-L functionals were used to calculate the binding energies, as shown in Table 1. The electron-donating groups (X = CH_3, NH_2 or OH) give high binding energies and the electron-withdrawing groups (X = CO_2Me or CN) give low binding energies. However, when the substituent group was made of halogen atoms, the opposite trend occurred. A Hammett plot of the binding energies, calculated using the M11-L functional, is shown in Scheme 4, in which the K_X and K_H are the equilibrium constant of the binding reaction of substituted and unsubstituted benzene respectively. The positive slope of σ(p), which is Hammet constant,[49-50] indicated that the electron-donating groups on complex **16** had higher binding energies when complex **16** was coordinated with graphene model **3**. However, the low R^2 revealed that some substituent groups did not follow this rule.

Table 1. The calculated binding energies of graphene model **3** with complex **16** using the B3LYP and M11-L functionals. The values are given in kcal/mol.

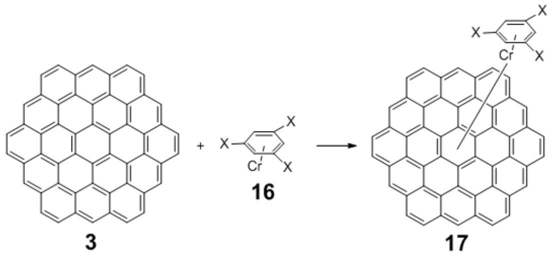

3 **16** **17**

X / Method	B3LYP	M11-L	σ(p)
H	31.7	41.8	0.00
CH_3	36.2	50.8	−0.07
NH_2	35.6	49.5	−0.16
OMe	33.1	51.4	0.12
F	35.9	43.6	0.34
Cl	24.6	40.1	0.37
Br	23.0	38.2	0.39
CO_2M	25.5	45.0	0.37
CN	27.9	42.6	0.56

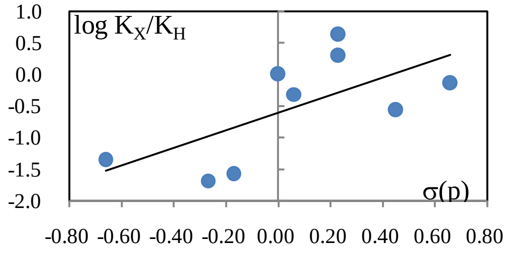

Scheme 4. The Hammett plot of the binding energies calculated using the M11-L functional. The calculated relative binding equilibrium constant could be described by log K_X/K_H = 1.39 σ(p) – 0.60 and R2 = 0.43.

As shown in Figure 3, graphene models **18** and **19** were used to explore the arrangement of coordinated $(CO)_3Cr$ and $(C_6H_6)Cr$. In model **18**, when one $Cr(CO)_3$ fragment was coordinated at position a, the binding energy of another $(CO)_3Cr$ fragment at position c was 24.5 kcal/mol. The binding energies for $(CO)_3Cr$ at positions d, e or f were 27.1 kcal/mol, 27.8 kcal/mol and 28.5 kcal/mol, respectively, which were about 3–**4** kcal/mol higher than that at position c because the repulsion between two neighboring $Cr(CO)_3$ fragments is larger when the second $Cr(CO)_3$ fragment is at position c. This result indicated that, if the distance between two neighboring $Cr(CO)_3$ fragments was more than three units, there were no interactions evident between the two neighboring $Cr(CO)_3$ fragments, however the closest distance between two neighboring $Cr(CO)_3$ fragments has not been reported experimentally.[41] Figure 3 shows that model **19** also followed the same rule. When one $(C_6H_6)Cr$ fragment was coordinated with the graphene model at position a, the binding energy of another $(C_6H_6)Cr$ fragment at either position d, e or f was about 7–8 kcal/mol higher than that at position c.

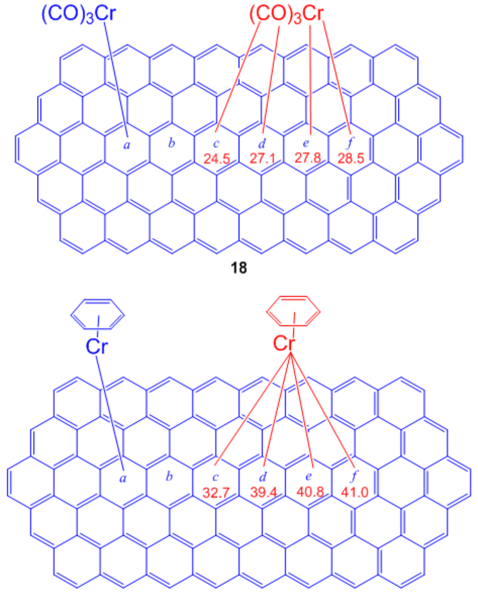

Figure 3. The M11-L binding energies of a second fragment of either $(CO)_3Cr$ or $(C_6H_6)Cr$ on the chromium coordinated graphene model. The values are given in kcal/mol.

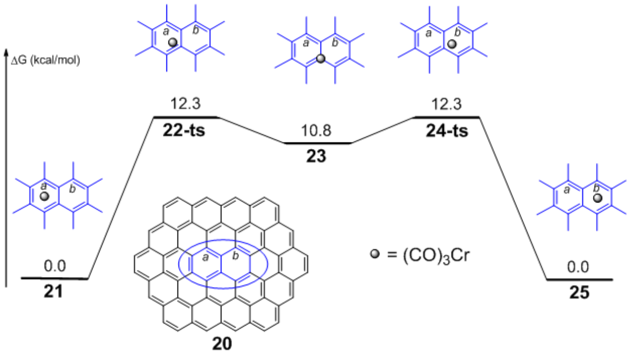

Scheme 5. The free energy profile for the migration of (CO)3Cr fragment calculated using the M11-L functional.

As shown in Scheme 5, oligoacene **20** was chosen as the graphene model to study the migration of a $(CO)_3Cr$ fragment on a graphene surface. The intermediate **21** was formed by the η6-coordination of oligoacene, **21** with the $(CO)_3Cr$ fragment and was set relative to zero for the free energy profile. The η^1-coordinated intermediate, **23** was formed with a 10.8 kcal/mol free energy increase via a η^3-coordinated transition state, **22-ts**. The barrier for this step was 12.3 kcal/mol. For the η6-coordinated complex 25, in which the $(CO)_3Cr$ fragment migrated from unit a to unit b, could be formed by the isomerization of intermediate **23** via the transition state **24-ts**. The overall barrier for the migration of the $(CO)_3Cr$ fragment to a neighboring unit was 12.3 kcal/mol, which was about 8 kcal/mol lower than the coordination energy of the $(CO)_3Cr$ fragment with graphene. The lower migration barrier indicated that the movement of the $(CO)_3Cr$ fragment on the graphene surface was easy. This result is consistent with the experimental observations.[39]

Conclusions

DFT calculations with the newly reported M11-L functional were performed to study the coordination of $(C_6H_6)Cr$ and $(CO)_3Cr$ fragments with graphene. Oligoacenes were chosen to model graphene and the binding energies of the $(C_6H_6)Cr$ and $(CO)_3Cr$ fragments indicated that when the radii of the centrosymmetric oligoacenes were larger than 3 unit, graphene could be modeled by oligoacenes to study the reactivities of the coordination with metal fragments. The meta-trisubstituted benzene coordinated chromium fragment was chosen to study the electronic effects. The Hammett plot showed that the electron-withdrawing substituent groups on the chromium fragments were favorable for the coordination of chromium fragments with graphene. The barrier for the migration of the $(CO)_3Cr$ fragment to a neighboring unit was low, therefore the $(CO)_3Cr$ fragment could freely move on the graphene surface. The closest distance between two neighboring Cr fragments on the same surface was three units.

Acknowledgements

This project was supported by the National Science Foundation of China (Grants 51302327 and 21372266).

Notes and references

[a] *School of Chemistry and Chemical Engineering, Chongqing University, Chongqing, China. E-mail: lanyu@cqu.edu.cn*

[b] *Department of Emergency, First Hospital, Jilin University, Changchun, China.*

† Electronic Supplementary Information (ESI) is available: The cartesian coordinates and energies of all of reported structures and the full authorship for GAUSSIAN 09. See DOI: 10.1039/b000000x/

1 A. K. Geim, K. S. Novoselov, Nat. Mater, 2007, 6, 183-191.
2 M. J. Allen, V. C. Tung, R. B. Kaner, Chem. Rev., 2010, 110, 132-145.
3 K. S. Novoselov, A. K. Geim, S. V. Morozov, D. Jiang, Y. Zhang, S. V. Dubonos, I. V. Grigorieva, A. A. Firsov, Science, 2004, 306, 666-669.
4 Y. b. Zhang, Y.W. Tan, H. L. Stormer, P. Kim, Nature, 2005, 438, 201-204.
5 F. Miao, S. Wijeratne, Y. Zhang, U. C. Coskun, W. Bao, C. N. Lau, Science, 2007, 317, 1530-1533.
6 A. H. Castro Neto, F. Guinea, N. M. R. Peres, K. S. Novoselov, A. K. Geim, Rev. Mod. Phys., 2009, 81, 109-162.
7 K. S. Novoselov, A. K. Geim, S. V. Morozov, D. Jiang, M. I. Katsnelson, I. V. Grigorieva, S. V. Dubonos, A. A. Firsov, Nature, 2005, 438, 197–200.
8 M. I. Katsnelson, K. S. Novoselov, A. K. Geim, Nat. Phys., 2006, 2, 620–625.
9 H. Liu, Y. Liu, D. Zhu, J. Mater. Chem., 2011, 21, 3335-3345.
10 V. Georgakilas, M. Otyepka, A. B. Bourlinos, V. Chandra, N. Kim, K. C. Kemp, P. Hobza, R. Zboril, K. S. Kim. Chem. Rev. 2012, 112, 6156-6214.
11 P. A. Denis, F. Iribarne, Int. J. Quantum Chem., 2010, 110, 1764-1771.
12 A. V. Titov, P. Král, R. Pearson, ACS Nano, 2010, 4, 229-234.
13 M. J. Allen, V. C. Tung, R. B. Kaner, Chem. Rev., 2010, 110, 132-145.
14 C. Mathieu, N. Barrett, J. Rault, Y. Y. Mi, B. Zhang, W. A. de Heer, C. Berger, E. H. Conrad, O. Renault, Phys. Rev. B, 2011, 83, 235436-1-235436-11.
15 R. C. Haddon, Tetrahedron Lett, 1980, 21, 1191-1192.
16 S. Sarkar, E. Bekyarova, R. C. Haddon, Acc. Chem. Res., 2012, 45, 673-682.
17 S. Sarkar, E. Bekyarova, S. Niyogi, R. Haddon, J. Am. Chem. Soc., 2011, 133, 3324-3327.
18 X. Zhong, J. Jin, S. Li, Z. Niu, W. Hu, R. Li, J. Ma, Chem. Commun., 2010, 46, 7340-7342.
19 M. Quintana, K. Spyrou, M. Grzelczak, W. R. Browne, P. Rudolf, M. Prato, ACS Nano, 2010, 4, 3527-3533.
20 V. Georgakilas, A. B. Bourlinos, R. Zboril, T. A. Steriotis, P. Dallas, A. K. Stubos, C. Trapalis, Chem. Commun., 2010, 46, 1766-1768.
21 T. A. Strom, E. P. Dillon, C. E. Hamilton, A. R. Barron, Chem. Commun., 2010, 46, 4097-4099.
22 J. R. Lomeda, C. D. Doyle, D. V. Kosynkin, W. F. Hwang, J. M. Tour, J. Am. Chem. Soc., 2008, 130, 16201-16206.
23 E. Bekyarova, M. E. Itkis, P. Ramesh, C. Berger, M. Sprinkle, W. A. de Heer, R. C. Haddon, J. Am. Chem. Soc., 2009, 131, 1336-1337.
24 R. Sharma, J. H. Baik, C. J. Perera, M. S. Strano, Nano Lett., 2010, 10, 398-405.
25 F.M. Koehler, A. Jacobsen, K. Ensslin, C. Stampfer, W. J. Stark, Small, 2010, 6, 1125-1130.
26 S. Niyogi, E. Bekyarova, M. E. Itkis, H. Zhang, K. Shepperd, J. Hick, M. Sprinkle, C. Berger, C. N. Lau, W. A. deHeer, E. H. Conrad, R. C. Haddon, Nano Lett., 2010, 10, 4061–4066.
27 X. L. Li, H. L. Wang, J. T. Robinson, H. Sanchez, G. Diankov, H. J. Dai, J. Am. Chem. Soc., 2009, 131, 15939-15944.
28 S. Dubin, S. Gilje, K. Wang, V. C. Tung, K. Cha, A. S. Hall, J. Farrar, R. Varshneya, Y. Yang, R. B. Kaner, ACS Nano, 2010, 4, 3845-3852.
29 P. K. Ang, S. Wang, Q. L. Bao, J. T. L. Thong, K. P. Loh, ACS Nano, 2009, 3, 3587-3594.
30 D. C. Marcano, D. V. Kosynkin, J. M. Berlin, A. Sinitskii, Z. Z. Sun, A. Slesarev, L. B. Alemany, W. Lu, J. M. Tour, ACS Nano, 2010, 4, 4806-4814.
31 S. Ryu, M. Y. Han, J. Maultzsch, T. F. Heinz, P. Kim, M. L. Steigerwald, L. E. Brus, Nano Lett., 2008, 8, 4597-4602.
32 D. C. Elias, R. R. Nair, T. M. G. Mohiuddin, S. V. Morozov, P. Blake, M. P. Halsall, A. C. Ferrari, D. W. Boukhvalov, M. I. Katsnelson, A. K. Geim, K. S. Novoselov, Science, 2009, 323, 610-613.
33 S. B. Bon, L. Valentini, R. Verdejo, J. L. G. Fierro, L. Peponi, M. A. Lopez-Manchado, J. M. Kenny, Chem. Mater., 2009, 21, 3433-3438.
34 F. Withers, M. Dubois, A. K. Savchenko, Phys. Rev. B: Condens. Matter Mater. Phys, 2010, 82, 073403-1-07403-4.
35 J. Zhou, Q. F. Liang, J. M. Dong, Carbon, 2010, 48, 1405-1409.
36 S. H. Cheng, K. Zou, F. Okino, H. R. Gutierrez, A. Gupta, N. Shen, P. C. Eklund, J. O. Sofo, J. Zhu, Phys. Rev. B: Condens. Matter Mater. Phys, 2010, 81, 205435-1-205435-5.
37 K. T. Chan, J. B. Neaton, M. L. Cohen, Phys. Rev. B: Condens. Matter Mater. Phys., 2008, 77, 235430-1-235430-12.
38 R. Zan, U. Bangert, Q. Ramasse, K. S. Novoselov, Nano Lett., 2011, 11, 1087-1092.
39 R. Zan, U. Bangert, Q. Ramasse, K. S. Novoselov, J. Phys.: Conf. Ser., 2012, 371, 012069-012072.
40 E. Bekyarova, M. E. Itkis, P. Ramesh, R. C. Haddon, Phys. Status Solidi RRL, 2009, 3, 184-186.
41 S. Sarkar, S. Niyogi, E. Bekyarova, R. C. Haddon, Chem. Sci., 2011, 2, 1326-1333.

42 M. J. Frisch, et al. Gaussian 09, revision A.02; Gaussian, Inc.: Wallingford, CT, 2009.
43 A. D. Becke, Phys. Rev. A, 1988, 38, 3098-3100.
44 C. Lee, W. Yang, R. G. Parr, Phys. Rev. B, 1988, 37, 785-789.
45 M. Dolg, U. Wedig, H. Stoll, H. Preuss, J. Chem. Phys., 1987, 86, 866-872.
46 P. Schwerdtfeger, M. Dolg, W. H. E. Schwarz, G. A. Bowmaker, P. D. W. Boyd, J. Chem. Phys., 1989, 91, 1762-1774.
47 Y. Zhao, D. G. Truhlar, Theor. Chem. Acc., 2008, 120, 215-241.
48 Y. Zhao, D. G. Truhlar, J. Phys. Chem. C, 2008, 112, 6860-6868.
49 L.P. Hammett. J. Am. Chem. Soc., 1937, 59, 96–102.
50 C. Hansch, A. Leo, R. W. Taft, Chem. Rev., 1991, 97, 165-195.